THE METASCIENCE **Volume 3, Issue 1 (Jan-Mar)-2025**
(An International Multidisciplinary Research Journal)

Sensor Application of Co-Polymer of Pyrrole and Aniline for Volatile Organic Compounds: A DFT Study

Mehboob Khan[1*], Rizwan Asghar[1], Sadiq ur Rehman[2], Khalid Raza[3], Saeed Anwar[4]
[1]Department of Chemistry, Hazara University Mansehra, PAKISTAN
[2]Kohat University of Science and Technology, Kohat, PAKISTAN
[3]State Key Laboratory of Advanced Technology for Materials Synthesis and Processing, Wuhan University of Technology, CHINA
*Corresponding Author Email: mehboobch22017@gmail.com

Keywords

Co-Polymer of Pyrroleaniline
Density Functional Theory
Sensors
Volatile Organic Compounds

ABSTRACT

Density functional theory calculations are performed to evaluate the sensing ability of co-polymer of pyrrole aniline for volatile organic compounds (VOCs). Interaction energies of PPA-X (X = Cl2, NH3, SO3, CH2O and HF) are calculated at B3LYP/6-31G (d) levels of theory and compared with the high level calibrated method (M05-2X/aug-cc-pVDZ). B3LYP/6-31G (d) gives the best correlation with the high level calibrated method. Interaction of oligopyrroleaniline with analytes shows a significant effect on the geometric and electronic properties; the conjugation is increased in the pyrroleanilineoligomers and movement of charge is increased over the polymeric backbone. The charge is transferred from analytes to pyrroleaniline oligomers and a more pronounced effect of charge transfer is observed in the case of sulphur trioxide (SO3) compared to Cl2, NH3, CH2O and HF. In nPA@SO3, the charge is transferred from polymer to analyte. This transfer of charge indicates the n-type doping effect of analytes. The HOMO- LUMO gap decreases after interaction with analytes, which results in a drop of resistance (conductivity increases). These theoretical outcomes are consistent with the experimental results; co-polymer of pyrroleaniline has more sensing ability toward the sulphure trioxide (SO3).

Introduction

Delocalization is a key factor that leads conjugated organic polymers (COPs) toward unique metal and polymer like prop- erties, including conductivity, processability, low density, and corrosion resistance [1, 2].Due to combined metal and polymer like properties, conjugated polymers have been introduced as interesting materials in the field of electronics, such as batteries [3], fuel cells, solar cells [4], sensors [5–7],electromagnetic shielding, smart windows [8], electro-catalysis [9],electroluminescence[10],and actuators .Among COPs, pyrrole(Py) and aniline (An) has gained much interest due to its low cost, high efficiency (for solar cells, sensors, electrochemical capacitance, photothermal agent), versatile redox properties, low response time, enhanced conductivity, and ease of preparation [11]. PPy and PAn can be synthesized either in a chemical or electrochemical way [12]. In chemical synthesis, the reaction of monomer with excess quantity of an oxidant (typically FeCl3) occurs at constant stirring in the presence of solvent [13, 14]. However, in electrochemical polymerization, counter and reference electrodes are placed in a solution of monomer and electrolyte (dopant). After applying an appropriate potential, the polymerization starts instantaneously at the working electrode. The electrochemical polymerization is preferred because it leads to simple and direct formation of good quality films with high electrical conductivity [11, 12, and 15]. This property makes PPy and PAn films highly suitable for applications in electronic devices. PPy has gained much attention as an electronic monitoring device in the area of drug delivery [16, 17] and sensors [18] while polyaniline (PANi) are built up of circuit board of electrical appliances, electrostatic discharge coating, and rust

protection [14]. Various Polyaniline based materials like N-doped carbon are prepared for heat treatment [15]. Now a day's Sensors based on Polyaniline gained a lot of attention for extensive use. Conducting polypyrrole plays a key role in the fabrication and testing of new DNA based drugs and proteins [7]. Polypyrrole (PPy) and polyaniline (PAn) are both of the most passive materials for the synthesis of nano composites and modeling bio analytical sensors [12]. Its applications clearly demonstrate its versatility and suitability for synthesizing various catalytic sensors and bio sensors [17]. Experimentally, a variety of analytes including H2O [19], CO [20], CO2 [21], SO2, NH 3 [22], CH4[19],NO2−[23],NO3−[24],NO2 [25], and NO are studied through PPy and PAn based sensors. However, the theoretical explanation for the sensing behavior of PPy and PAn toward different analytes remained insufficient and is limited to few analytes [26–29]. Recently, we reported the sensing ability of PPy and PAn for nitrate ion (NO3−), sulphur dioxide (SO3), ammonia (NH3) etc in both gas and aqueous phases [30]. Based on those results, we continued our study with SO3, NH3, CH2O, HF. Volatile organic compounds (VOCs) are the products of combustion of fuels, their emission is dominated by transportation related sources [31].

In environmental science, VOCs are very toxic. Toxic Chemicals are those "which in an adequate quantity can even cause death or damage to organs, DNA and cells tissues, upon a chemical reaction, when an organism is exposed to them." [1] Agriculture Industry and other industries use toxic chemicals apart from their toxicity. The majorities of toxic industrial chemicals have linked material safety data sheets as well as are categorized as harmful substances. Pesticides are harmful to different animals, insects, and also for pests (Mice, cockroaches). The existence of toxic gases molecules such as Cl2, NH3, and SO3 in the environment is extremely harmful for human health. These toxic chemicals that we might come in contact with them in our daily life. It is likely to encounter toxic chemicals in numerous areas as an effect of exhaust gases manufacturing mass effluents, emitted by mechanical vehicles, and fossil fuels ignition for heating. For the detection of these toxic chemicals Sensor systems play a significant role in the field of agriculture, food industry, and health. For developing accurate sensor system, we need easily producible, highly selective, and more sensitive material. Optical and electrochemical characteristics of conductive polymers are extremely suitable material for sensor system usage. Conducting polymers are important probes to monitor the quantity of VOCs in the air. Among conducting polymers, polypyrrole is an excellent material as a sensor for VOCs analytes. In this report, we aim to get theoretical insight into the sensor mechanism of polypyrrole and polyaniline for VOCs molecules and anions. In this study, we examine the geometrical structures of PPy and PAn before and after interaction with Cl2, NH3, SO3, CH2O and HF. Furthermore, FMOs, charge (Mulliken and natural bonding orbital (NBO), and spectroscopic (UV and IR) analyses are also performed and the results are compared with available experimental data.

Computational details

All calculations are performed with Gaussian 09, while results are analyzed through Gauss View 5.0. Based on our previous study with CoPPyAn- NO3- a high-level calibrated method M05-2X/aug-cc- pVDZ is used to find the interaction energies of 1 CoPPyAn -X (SO3, Cl2, FD, HF and NH3). The interaction energies with M05-2X/aug-cc-pVDZ give the standard values that are fur- ther compared with the interaction energies calculated with B3LYP-CP/6-31G (d) and B3LYP/6-31G (d). The electronic properties (HOMO, LUMO, IP, EA, energy gap), charge transfer, and spectroscopic (UV-vis) properties of Co-polymer of Pyrrole and

aniline (1, 2, 3) oligomers and their complexes are calculated at B3LYP/6-31G(d) because it gives the best estimations that are comparable to experimental results [28, 30].

Table 1 Optimized important geometric parameters of CoPPyAn -X (SO3, Cl2, FD, HF and NH3).

COMPLEXES	dN20-H22(Å)	dX24-H22 (Å)	∠C4N5C15	∠N20H22X24
1PA	1.01		109.80	
1PA@Cl2	1.02	2.77	109.71	115.15
1PA@NH3	1.03	2.06	109.70	114.33
1PA@SO3	1.04	2.87	110.71	114.53
1PA@CH2O	1.02	2.16	109.70	116.52
1PA@HF	1.02	2.19	108.01	116.72
2PA	1.01		109.80	
2PA@Cl2	1.03	2.75	109.70	115.10
2PA@NH3	1.04	1.98	109.65	114.21
2PA@SO3	1.06	2.55	109.70	114.81
2PA@CH2O	1.03	2.15	109.67	116.15
2PA@HF	1.04	2.13	107.50	119.15
3PA	1.01		109.80	
3PA@Cl2	1.05	2.72	109.65	115.09
3PA@NH3	1.04	1. 97	109.62	115.90
3PA@SO3	1.07	2.39	109.65	115.10
3PA@CH2O	1.05	2.06	109.64	116.01
3PA@HF	1.06	3.231	107.48	117.73

Results and Discussion

Geometry optimization

Geometry optimization is an important process that generates the lowest (stable) energy. Geometries of CoPPyAn oligomers with SO3, Cl2, FD, HF and NH3 are optimized. All the possible geometries of CoPPyAn with analytes (SO3, Cl2, FD, HF and NH3) are optimized and given in Figs. S1-S2 (Supporting information). The optimized parameters including bond length, bond angle, and dihedral angles are given in Table 1. The numbering schemes of nCoPPyAn -X (SO3, Cl2, FD, HF and NH3) are given in Figs. 1a and b, respectively.

nCoPPyAn-Cl2

Geometry of isolated copolymer of pyrrole aniline changes after interaction with chlorine gas. The optimized geometry of nCoPPyAn- Cl2 is depicted in Fig. 2. In all oligomers of copolymer of pyrrole aniline nCoPPyAn (n= 1, 2, 3), the N−H bond distance (dN20-H22) is 1.01 Å. After interaction with chlorine molecule (Cl2), the bond distance (dN20-H22) increases to 1.05 Å. The N−H bond distance increases as the number of oligopyrroleaniline unit's increase. The intermolecular distance (dCl24-H22) in 1PA@Cl2 is 2.77 Å, which decreases to 2.72 Å in which 2PA@Cl2 is 2.75 and 3PA@Cl2 is 2.72, shows different behavior than other oligopyrroleanilines because the lowest energy structure is the one in which the Cl2 gas molecules interacts with the terminal pyrrole ring rather than the central one. Moreover, in higher oligomers (3PA@Cl2) the stable structures are those in which the Cl2 gas molecules interacts with the central pyrrole ring. The bond distance (dCl24-H22) decreases as the size of oligomers increases, which indicates stronger interaction of nCoPPyAn (n= 1, 2, 3) with Cl2 gas molecules.

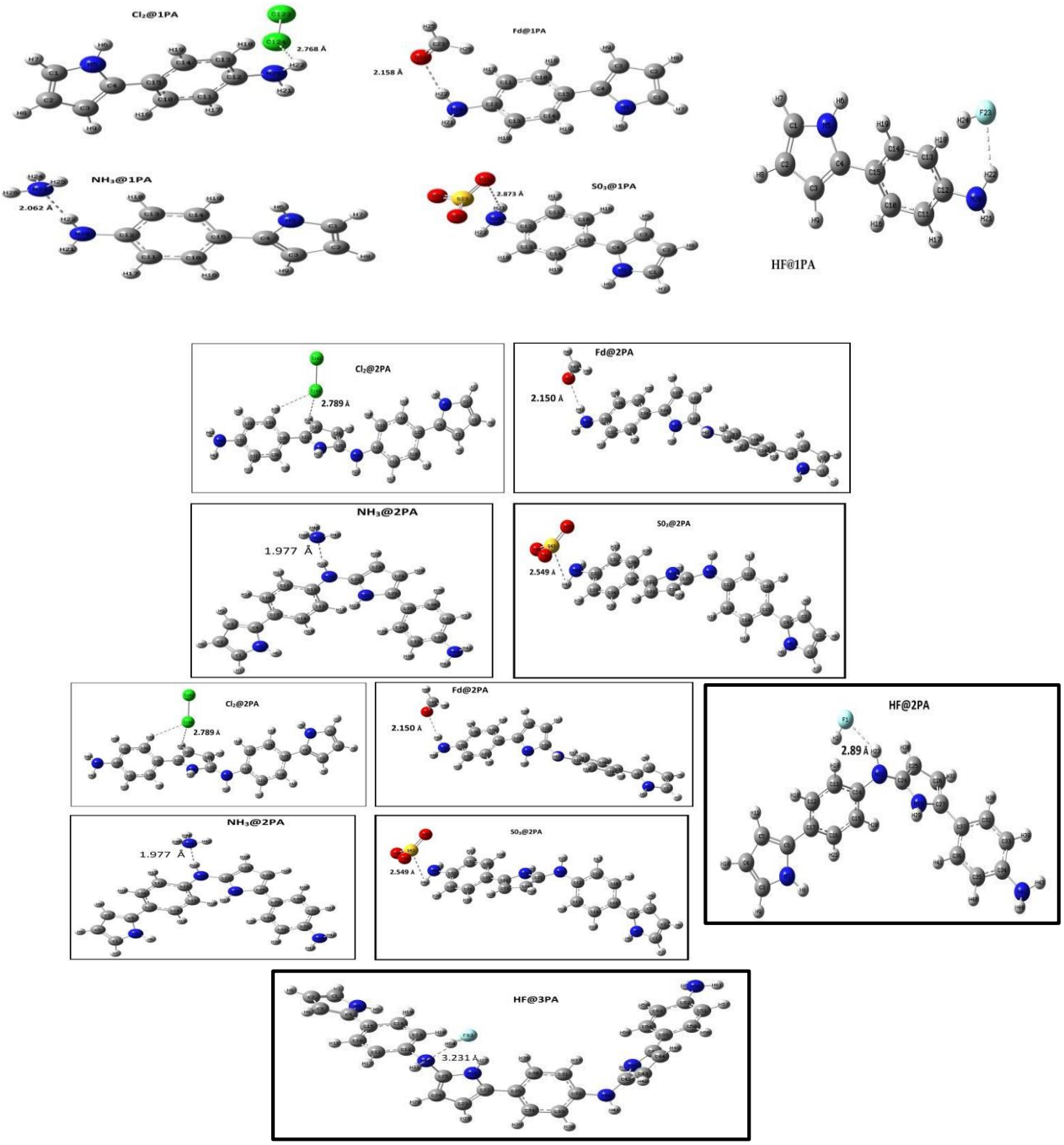

Fig. 1 Optimized geometries and interaction distance in nCoPPyAn@X

The bond angle or bridging angle ∠C4N5C15 in the isolated copolymer of pyrrole and aniline ring is 109.80° and is reduced to 109.71° in 1PA@Cl2 complex. However, in 2PA, the bond angle ∠ C4N5C15 is 109.70° and after complexation with chlorine gas molecule, the bond angle decreases to 109.65°. The reduction of bond angle in 3PA@Cl2 and higher oligomer is more pronounced. The reduction in bond angle is attributed to the influence of the ring adjacent to the central ring (in higher oligomer). The decrease in the bond angle increases the flow of charge throughout the polymeric skeleton. The second bridging angle ∠N20H22Cl24 is 115.15° in 1PA@Cl2, 115.10° in 2PA@Cl2, 115.09° in 3PA@Cl2. The reduction in

bridging angle ∠N20H22Cl24 is supposed to arise from the interaction of chlorine gas molecules and pyrroleaniline oligomers. The enhanced interaction of nPA and Cl2 not only affects the bond angle and bond energies but also causes changes in the dihedral angle.

nCoPPyAn-NH3

The N−H bond distance (dN20-H22) is 1.01 Å in 1PA-NH3, which gradually increases to 1.03 Å (in 2PA@NH3) to 1.04 Å (In higher oligomers). The optimized geometries of nPA@NH3 are given in Fig. 3. The intermolecular distance (dN23-H22) in 1PA@NH3 is 2.06 Å, which decreases to 1.98 Å in 2PA@NH3 and 1. 97 Å in 3PA@NH3. The value of dN23-H22 in higher oligomers is almost comparable (see Table 1). The increase in N−H bond distance (dN20-H22) and decrease in intermolecular bond distance (dN23-H22) indicate the interaction between the nitrogen of NH3 and hydrogen of pyrrole as a result of hydrogen bonding. The bond angle or bridging angle ∠C4N5C15 in the isolated copolymer of pyrrole and aniline ring is 109.80° and is reduced to 109.70° in 1PA@NH3 complex. However, in 2PA, the bond angle ∠ C4N5C15 is 109.65° and after complexation with ammonia gas molecule, the bond angle decreases to 109.62°. The reduction of bond angle in 3PA@NH3 and higher oligomer is more pronounced.The decrease in angle ∠ C4N5C15 is due to the chain length elongation and the effect of neighboring pyrroleanilinerings. The bond angle ∠N20H22N24 is 114.33° in 1PA@NH3, 114.21° in 2PA@NH3 and 115.90° in 3PA@NH3. The increase in bond angle ∠ N20H22N24 indicates that the interaction of NH3 with the pyrroleaniline ring is less compared to the chlorine gas molecule.

nCoPPyAn-SO3

After interaction with sulphur trioxide (SO3), the N−H bond distances (dN20-H22) in all oligomers of pyrroleaniline are changed from 1.01 Å to 1.07 Å. The optimized geometries of nPA@SO3 are illustrated in Fig. 4. The bond distance (dS23-H22) in 1PA@SO3 is 2.87 Å and 2PA@SO3 is 2.55 Å, while in higher oligomers, the bond distance (dS23-H22) is 2.39 Å. The bond distance (dS23-H22) decreases with chain length elongation. The bond angle or bridging angle ∠C4N5C15 in the isolated copolymer of pyrrole and aniline ring is 109.80° and is reduced to 110.71° in 1PA@SO3 complex. However, in 2PA, the bond angle ∠ C4N5C15 is 109.70° and after complexation with sulphur trioxide gas molecule, the bond angle decreases to 109.65°. The reduction of bond angle in 3PA@Cl2 and higher oligomer is more pronounced. The reduction in bond angle is attributed to the influence of the ring adjacent to the central ring (in higher oligomer). The decrease in the bond angle increases the flow of charge throughout the polymeric skeleton the bond angle ∠N20H22S24 is 114.53° in 1PA@SO3, 114.81° in 2PA@SO3 and 115.10° in 3PA@SO3. a similar trend is observed in higher oligomers.

nCoPPyAn-CH2O

After interaction with farmaldehyde (CH2O), the N−H bond distances (dN20-H22) in all oligomers of pyrroleaniline are changed from 1.01 Å to 1.05 Å. The optimized geometries of nPA@CH2O are illustrated in Fig. 4. The bond distance (dO23-H22) in 1PA@CH2O is 2.16 Å and 2PA@CH2O is 2.15 Å, while in higher oligomers, the bond distance (dS23-H22) is 2.06 Å. The bond distance (dS23-H22) decreases with chain length elongation. The bond angle or bridging angle ∠C4N5C15 in the isolated copolymer of pyrrole and aniline ring is 109.80° and is reduced to 109.70° in 1PA@NH3 complex. However, in 2PA, the bond angle ∠ C4N5C15 is 109.67° and after complexation with ammonia gas molecule, the bond angle

decreases to 109.64°. The reduction of bond angle in 3PA@NH3 and higher oligomer is more pronounced. The decrease in angle ∠ C4N5C15 is due to the chain length elongation and the effect of neighboring pyrroleanilinerings. The bond angle ∠N20H22O24 is 116.52° in 1PA@CH2O, 116.15° in 2PA@CH2O and 117.01° in 3PA@CH2O. a similar trend is observed in higher oligomers.

nCoPPyAn-HF

After interaction with hydrogen floride (HF), the N−H bond distances (dN20-H22) in all oligomers of pyrroleaniline are changed from 1.01 Å to 1.06 Å. The optimized geometries of nPA@HF are illustrated in Fig. 1. The bond distance (dF23-H22) in 1PA@HF is 2.19 Å and 2PA@HF is 2.13 Å, while in higher oligomers, the bond distance (dF23-H22) is 3.231 Å. The bond distance (dF23-H22) decreases with chain length elongation. The bond angle or bridging angle ∠C4N5C15 in the isolated copolymer of pyrrole and aniline ring is 109.80° and is reduced to 108.01° in 1PA@HF complex. However, in 2PA, the bond angle ∠ C4N5C15 is 107.50° and after complexation with ammonia gas molecule, the bond angle decreases to 107.48°. The reduction of bond angle in 3PA@HF and higher oligomer is more pronounced. The decrease in angle ∠ C4N5C15 is due to the chain length elongation and the effect of neighboring pyrroleanilinerings. The bond angle ∠N20H22F24 is 116.72° in 1PA@HF, 116.15° in 2PA@HF and 117.73° in 3PA@HF. A similar trend is observed in higher oligomers. On the basis of geometric parameters (bond length and angle), it is clear that the response of oligopyrroleaniline toward molecule analyte (SO3) is greater compared to other gaseous molecular analytes (Cl2, NH3 and CH2O). In nPA@SO3 the interaction occurs between the oxygen of SO3 analyte and hydrogen of the pyrrole ring. Both the oxygen atoms play a role in the formation of a strong hydrogen bond.

Interaction energies

In our previous work, the interaction energies of nPy-NO3− are simulated at methods calibrated against CCSD (T) includ- ing, M05-2X/aug-cc-pVDZ, M06-2X/aug-cc-pVDZ, B97- D3/aug-cc-pVTZ, and B97XD/aug- cc-pVTZ. The resulted interaction energies from these methods were evaluated against the interaction energies of some routinely used methods. B3LYP-CP and B3LYP-DCP performed best, and the results were quite comparable to the standard calibrated methods. Therefore, the interaction energies in this study are calculated at B3LYP-CP/6-31G (d) and M05-2X/aug-cc- pVDZ levels of theory [30]. The interaction energies are also calculated at B3LYP/6-31G (d) for comparison purposes. The interaction energies are calculated by using the following equation.

$$\Delta E = E\ Complex - (EPPA + E\ Analytes)$$

The interaction energies of nPA-X (Cl2, NH3, SO3 and CH2O) are given in Table 2, while the graphical comparison of inter- action energies is illustrated in Fig. 5.

nCoPPyAn-Cl2

Initially, the interaction energies of nPA with chlorine (Cl2) ion are simulated at the calibrated method (M05-2X/aug-cc- pVDZ) to estimate the error in commonly used B3LYP/6- 31G (d) level of theory. The interaction energy of the monomer of pyrroleabiline (PA) and chlorine molecule (Cl2) at M05-2X/aug-cc- pVDZ is −18.78 kcal mol−1. However, the interaction energies for 1PA@Cl2 at B3LYP/ 6-31G (d) is – 9.80 kcal mol−1. The high difference between M05-2X and the B3LYP/6-31G (d) for 1PA@Cl2 is probably due to the charged(e) nature of the chlorine gas analyte where the electrostatic component is overestimated. The interaction energy calculated at B3LYP/6-31G (d) shows an error of almost 8 kcal mol−1 (≈ 40%). At B3LYP/6-31G (d), the interaction energy of 2PA with Cl2 in 2PA@Cl2 complex is −10.08 kcal mol−1, which increases to −11.26 kcal mol−1 in 3PA@Cl2 complex. The interaction energies increase as the size of oligopyrroleaniline increases. This increase is due to the delocalization of π-electrons over the pyrrole and aniline rings and strong interaction between the analyte (Cl2) and oligopyrrole and aniline.

Table 2: Comparison between interaction energies (kcal mol−1) of nPA@X (X: Cl2, NH3, SO3, CH2O and HF) at B3LYP/6-31G (d) levels of theory

COMPLEXES	M05-2X/ aug-cc-pVDZ	B3LYP/6-31G (d)
1PA@Cl2	−18.78	– 9.80
2PA@Cl2		−10.08
3PA@Cl2		−11.26
1PA@NH3	−11.98	-6.83
2PA@NH3		-8.29
3PA@NH3		−8.65
1PA@SO3	−21.02	-20.57
2PA@SO3		-20.80
3PA@SO3		−20.95
1PA@CH2O	−19.55	-4.94
2PA@CH2O		-4.96
3PA@CH2O		−6.57
1PA@HF	−18.55	-7.97
2PA@HF		-8.06
3PA@HF		−15.19

nCoPPyAn-NH3

The interaction energy of 1PA with ammonia gas molecule (NH3) is −11.98 kcal mol−1 at M05-2X/aug-cc- pVDZ. The interaction energies 1PA@NH3, 2PA@NH3 and 3PA@NH3 at B3LYP/6-31G (d) level of theory are -6.83 kcal mol−1, -8.29 kcal mol-1 and −8.65 kcal mol−1, respectively. In this case, the difference in interaction energies at above three methods is relatively small, B3LYP/6-31G (d) shows a difference of about 3.13 kcal mol−1 from M05-2X/aug-cc-pVDZ. The difference in interaction energies may arise due to the neutral nature of analyte (NH3). The interaction energy increases as the chain length elongates, but the difference in interaction energy is more prominent in higher oligomers compared to the monomer of pyrroleaniline and ammonia gas complex.

nCoPPyAn-SO3

The interaction energy of 1PA with sulphur trioxide gas molecule (SO3) is −21.02 kcal mol−1 at M05- 2X/aug-cc-pVDZ. The interaction energies 1PA@SO3, 2PA@SO3 and 3PA@SO3 at B3LYP/6-31G (d) level of theory are -20.57 kcal mol−1, -20.80 kcal mol-1 and −20.95 kcal mol−1, respectively. In this case, the difference in interaction energies at above three methods is relatively small, B3LYP/6-31G (d) shows a difference of about 0.07 kcal mol−1 from M05-2X/aug-cc-pVDZ. The difference in interaction energies may arise due to the delocalization of pi electrons analyte (SO3). The interaction energy increases as the chain length elongates, but the difference in interaction energy is more prominent in higher oligomers compared to the monomer of pyrroleaniline and ammonia gas complex.

nCoPPyAn-CH2O

The interaction energy of 1PA with farmaldehyde (CH2O) is −19.55 kcal mol−1 at M05-2X/aug-cc-pVDZ. The interaction energies 1PA@CH2O, 2PA@CH2O and 3PA@CH2O at B3LYP/6-31G (d) level of theory are -4.94 kcal mol−1, -4.96 kcal mol-1 and −6.57 kcal mol−1, respectively. In this case, the difference in interaction energies at above three methods is relatively high, B3LYP/6-31G(d) shows a difference of about 12.98 kcal mol−1 from M05-2X/aug-cc-pVDZ. The difference in interaction energies may arise due to the stable configuration of analyte (CH2O). The interaction energy increases as the chain length elongates, but the difference in interaction energy and B3LYP/6-31G(d) is more prominent in higher oligomers compared to the monomer of pyrroleaniline and farmaldehyde complex.

nCoPPyAn-HF

The interaction energy of 1PA with hydrogen floride (HF) is −18.55 kcal mol−1 at M05-2X/aug-cc-pVDZ. The interaction energies 1PA@HF, 2PA@HF and 3PA@HF at B3LYP/6-31G (d) level of theory are -7.97 kcal mol−1, -8.06 kcal mol-1 and −15.19 kcal mol−1, respectively. In this case, the difference in interaction energies at above three methods is relatively moderate, B3LYP/6-31G (d) shows a difference of about 2.36 kcal mol−1 from M05-2X/aug-cc-pVDZ. The difference in interaction energies may arise due to the strong intermolecular force of analyte (HF). The interaction energy increases as the chain length elongates, but the difference in interaction energy and B3LYP/6-31G (d) is more prominent in higher oligomers compared to the monomer of pyrroleaniline and hydrogen floride complex. Interaction energies of higher oligomer show no trend in values. From the above discussion, it is clear that the ionic analyte (SO3) shows greater interaction than the other analytes (Cl2, NH3, CH2O and HF) due to strong hydrogen bonding and dual interaction with oligopyrroleaniline (1, 2 and 3).

Charge analysis (QNBO)

One more valuable factor of this study could be a charge transfer which might study for wide estimation of the interaction among isolated PA and analytes (toxic chemicals). Therefore, we have a tendency to know the number of charge transfers on the formation of complex by measuring the natural band orbital charge. B3LYP/6-31 G (d) is set to record NBO charges. With help of charge transfer measurement Sensing actions of pyrrol-aniline can be checked towards toxic chemicals (analytes) on the formation of complexes [27]. Positive value of charge transfer indicates segments (PA) gain charge from analytes, while negative charge transfer value is sign of transfer of charge from segments (PA) to analytes.To analyze alter in electronic properties, such as band gap λmax and HOMO, LUMO transfer of Charge

transfer (e-) is a reliable technique for the determination of sensing capabilities of PA.The structural representations of charge transfer QNBO are shown in Fig.2 Results are listed in table.3.

Table.3. Charge analysis (NBO) for analytes @PA complexes at B3LYP/6-31G (d)

Q_{NBO} ANALYSIS (e-)			
ANALYTES	**@1PA**	**@2PA**	**@3PA**
Cl_2	-0.225	-0.293	-0.225
FD	0.017	0.017	0.019
NH_3	0.034	0.042	0.04
SO_3	-0.256	-0.257	-0.395
HF	0.001	0.001	-0.027

From table.3 transfer of charge QNBO analysis give us an idea about the types of binding force between PA and analytes on account of which charge transfer occurs. Charge may be shifted towards analytes (Cl2, FD, NH3, SO3, and HF) or analytes to Segment (PA). Here we have some positive and negative values of transfer of charge. The results of QNBO charge analysis of all analytes (Cl2, FD, NH3, SO3, and HF) after interaction with PA are given in Table 7. Complex formations of PA-analytes were recognized due to the transfer of electrons from analytes to PA for FD, NH3, and reverse charge transfer occurs. as can be seen from the data listed in Table.5 In FD@1PA, FD@2PA ,and FD@3PA complexes, FD lose about 0.017, 0.017and 0.019 e− charges to 1PA,2PA,and 3PA, respectively, based on NBO charge analysis. Similarly in NH3@1PA, NH3@2PA, NH3@3PA, complexes NH3 lose about0.034, 0.042, and 0.04 e− charges to @1PA@2PA, 3PA, respectively. On the other hand, at Cl2@1PA, Cl2@2PA ,and Cl2@3PA complexes, Cl2 specie takes- 0.225, -0.293, and -0.225 e− charges from 1PA,2PA and 3PA based on NBO, and SO3@1PA, SO3@2PA,and SO3@3PAcomplexes SO3 takes -0.256, -0.257and -0.395e− charges from 1PA,2PA and 3PA based on NBO charge analysis respectively. The results transfer of charge as a matter of fact that the examined molecules serve as H-bond donors for FD, and NH3. In some complexes they are sowing character of H-bond acceptors. It may be viewed that highest transfer of charge associated with SO3. This coincides to the maximum interaction energy between all complexes tested. The amount of charge transfer ranges from -0.395 e- to 0.042 e- among Cl2, FD, NH3, SO3, HF @PA. The highest charge transfer (-0.256 e-, -0.257 e-, -0.395 e-) in the SO3@1PA, SO3@2PA and SO3@3PA complexes are unexpected with high interaction energies. charge transfer and interaction energies results indicate that PA shows high sensing ability towards Cl2 and SO3.The trends in sensing mechanism is: analytes@3PA > analytes@2PA > analytes@3PA.

Orbital analysis

The HOMO-LUMO distribution of analytes, isolated and complexes are shown in figure 5. Molecular orbital (MO) energies changes as a result of sensing of analytes. HOMO-LUMO energy varies due to overlapping of molecular orbital [28]. Using HOMO_LUMO values of energies, Energy gap (Eg) were obtained which can describe well sensing phenomena of pyrrole-aniline (PA) towards toxic chemical [29]. The electronic stabilities upon interactions can be determined by using HOMO-LUMO energy gap (Eg), which is a major parameter for differentiation. In general, the sensitivity as well as conductivity are inversely proportional to the Band gap (Eg) [f]. The HOMO-LUMO energies obtained .by means of TD-DFT level

of theory at basis sets i.e B3LYP/6-31 G(d) Results are shown in table 6 HOMO-LUMO energies of 1PA are -4.712ev and 0.034ev respectively. The band gap is 4.747ev. 1PA complexes of Cl2, FD, NH3, SO3, HF, determined Eg values are 2.607, 3.018, 4.731, 4.251, 4.547ev respectively, shows minute decline in (Eg) as consequences of this, sensitivity and conductivity also increases. SO3@1PA have -5.597, and -1.345ev values of HOMO-LUMO energies and band gap is 4.251ev enlightening 1PA possess greater sensitivity to sulfur trioxide (SO3). Results are listed in table.6. Isolated 2PA are have HOMO-LUMO energies values of -4.672 and -0.123ev and Eg is 4.549ev. A raise of 4.749, -4.581, 4.048, -4.840 and -4.634ev was calculated in energies of HOMO of 2PA on interaction with Cl2, FD, NH3, SO3 and HF, correspondingly. While decrease in the LUMO energy of 2PA with sulfur trioxide(SO3), the energy is -1.384ev and 2PA LUMO energies decreases upon interaction with Cl2, FD, NH3, SO3, HF, the energies decreases having values in that order -2.876,-1.673, -0.392, and - 0.394ev.In contrast to isolated PA and complexes, Analytes comprise elevated Eg value as the band gap rely on analytes nature, outcome of band gap on complex formation up to a certain extent varies from isolated PA.Typically in complex band gap variation occurred when analytes band gap altered minutely and we are able to detect it.The isolated 2PA having Eg value 4.549. For for 2PA complexes of Cl2, FD, NH3, SO3, HF, band gap is observed i.e. 1.869, 2.909, 3.656, 3.456 and 4.239ev respectively.

Table 4 HOMO-LUMO and Energy of Fermi level (EFL), and band gap (Eg) of Cl2, FD, NH3, SO3, HF @1PA, 2PA and 3PA complexes

S. No.	Analytes	E_{HOMO} (ev)	E_{LUMO}(ev)	E_{FL}(ev)	Eg(ev)
1.	Chlorine(Cl_2)	-8.522	-3.874	-6.204	4.648
2.	Farmaldehyde(FD)	-7.306	-1.146	-4.225	6.161
3.	Amonia(NH_3)	-6.869	2.139	0.726	9.007
4.	Sulphertrioxide (SO_3)	-9.459	-2.959	-20869	6.501
5.	HF	-4.946	-0.399	-2.673	11.915
6.	Pyrole-aniline monomer(1PA)	-4.712	0.034	-2.339	4.747
7.	Pyrole-aniline dimer(2PA)	-4.672	-0.123	-2.398	4.549
8.	Pyrole-aniline trimer(3PA)	-4.591	-0.159	-2.375	4.431
9.	Cl_2@1PA	-5.317	-2.711	-4.014	2.607
10.	FD@1PA	-4.629	-1.612	-3.121	3.018
11.	NH_3@1PA	-4.338	0.393	-1.973	4.731
12.	SO_3@1PA	-5.597	-1.345	-3.471	4.251
13.	HF@1PA	-4.946	-0.399	-2.673	4.547
14.	Cl2@2PA	-4.749	-2.876	-3.812	1.869
15.	FD@2PA	-4.581	-1.673	-3.127	2.909
16.	NH3@2PA	-4.048	-0.392	-2.220	3.656
17.	SO3@2PA	-4.840	-1.384	-3.111	3.456
18.	HF@2PA	-4.634	-0.394	-2.513	4.239
19.	Cl2@3PA	-4.894	-2.667	-3.780	2.227
20.	FD@3PA	-4.119	-1.595	-2.857	2.523
21.	NH3@3PA	-4.040	-0.093	-2.067	3.947
22.	SO3@3PA	-4.947	-1.577	-3.262	2.371
23.	HF@3PA	-4.672	-0.530	-2.601	4.142

When band gap of HF@2PA increases, it will result in decrease of conductivity and vice versa. While in case of Cl2@2PA, FD@2PA, NH3@2PA, SO3@2PA, and the band gap

reduction results in boost in conductivity or sensitivity. Likewise, HOMO-LUMO energies and band gap of an isolated 3PA are -4.59ev, -0.159ev and -4.431ev respectively. A minute difference in Eg exhibited by complexes of 1PA, 2PA and 3PA with mentioned analytes (Cl2, FD, NH3, SO3, HF,). While in case of Cl2@3PA**,** FD@3PA, NH3@3PA, SO3@3PA, HF@3PA, observed band gap values are -1.869, -2.909, -3.656, -3.456-and 4.239ev correspondingly. Eg value of 3PA with Cl2, FD and SO3, decreases which brings strong sensitivity for toxic chemicals (analytes). Observation revealed that analytes (Cl2, FD, NH3, SO3, HF,) have shown maximum response on the Eg value of 1PA, 2PA and 3PA. Results are depicted in figure 5. Cl2@2PA FD@2PA and SO3@2PA have small Eg values of about 1.869, 2.909 and 3.456ev, respectively. The sensing property of PA have shown improvement with, Cl2, FD, and SO3 than any other analytes. Among 1PA, 2PA, and 3PA, 3PA has highest sensitivity due to greater decrease in their band gap of anylytes@3PA complexes. The band gap energy of 3PA, 2PA and 1PA complexes follows descending order as analytes@3PA < analytes@2PA < analytes@1PA< isolated PA.

To sum up, we can say that the lowest band gap energies of analytes@3PA is the leading factor for greatest conductivity and sensitivity, whereas isolated PA shows opposite result as it has least conductivity and sensitivity due to increased band gap energies [30]. We can understand the sensing action of PA toward analytes by measuring the changes in potential energies of vacuum level and Fermi level, which tells us that least amount of energy is necessary for taking away one electron from the Fermi level to vaccum or [31]. The value of Fermi level of isolated 1PA changed from -2.339ev to -4.014-3.121, -1.973, -3.471 and -2.67311ev for for Cl2@1PA**,** FD@PA, NH3@1PA, SO3@1PA, HF@1PA While the value of 2PA is changed from --2.398 ev to -3.812, -3.127, -2.220, -3.111, and -2.513ev for Cl2@2PA**,** FD@2PA, NH3@2PA, SO3@2PA, HF@2PA. The 3PA changed from -2.375ev to -3.7803, -2.857, -2.067, -3.262, and-2.60182ev for Cl2@3PA**,** FD@3PA, NH3@3PA, SO3@3PA, HF@3PA, respectively. These all HOMO – LUMO structures of analytes (Cl2, FD, NH3, SO3, HF) are shown in Fig.(11,12)

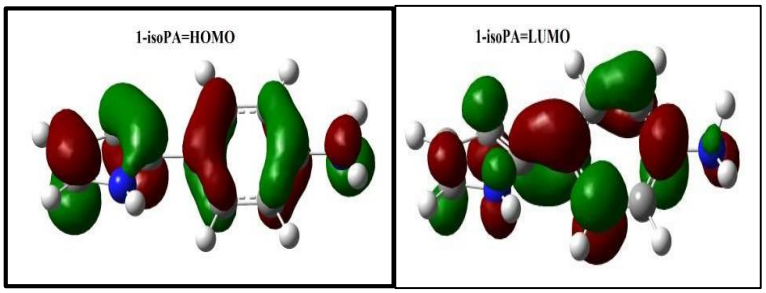

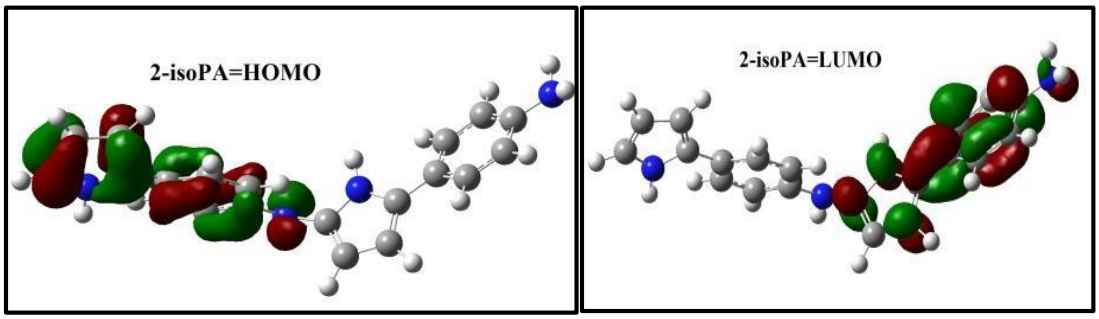
2-isoPA=HOMO
2-isoPA=LUMO

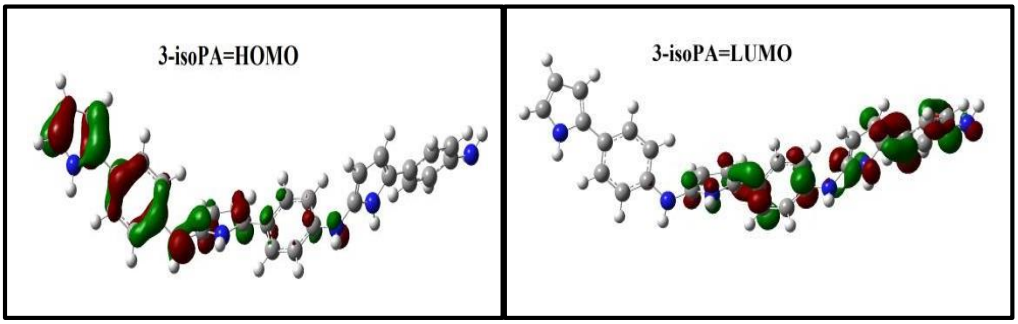
3-isoPA=HOMO
3-isoPA=LUMO

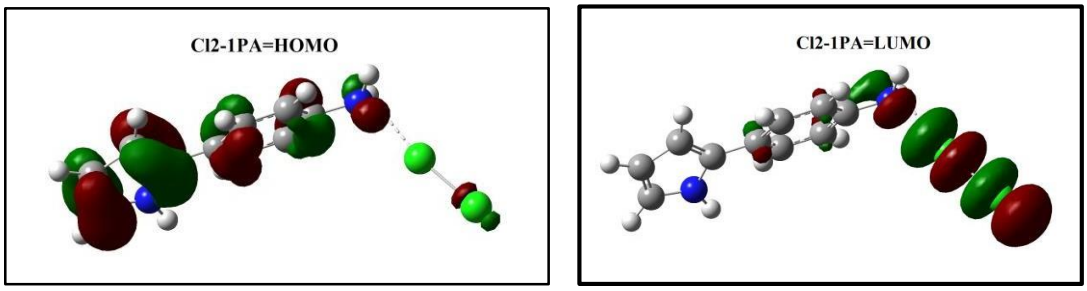
Cl2-1PA=HOMO
Cl2-1PA=LUMO

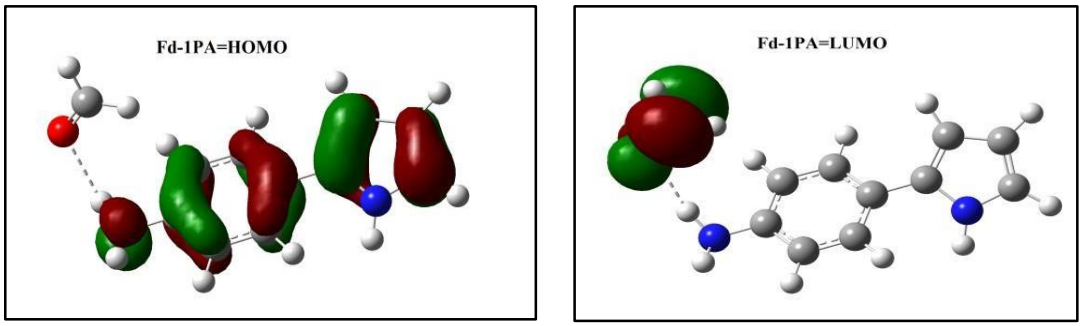
Fd-1PA=HOMO
Fd-1PA=LUMO

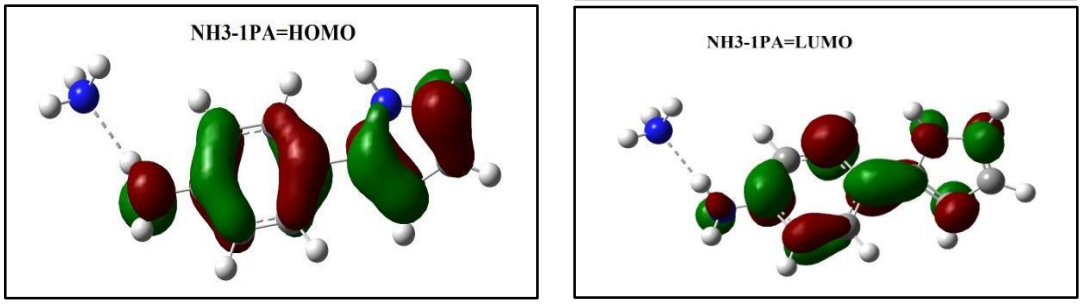
NH3-1PA=HOMO
NH3-1PA=LUMO

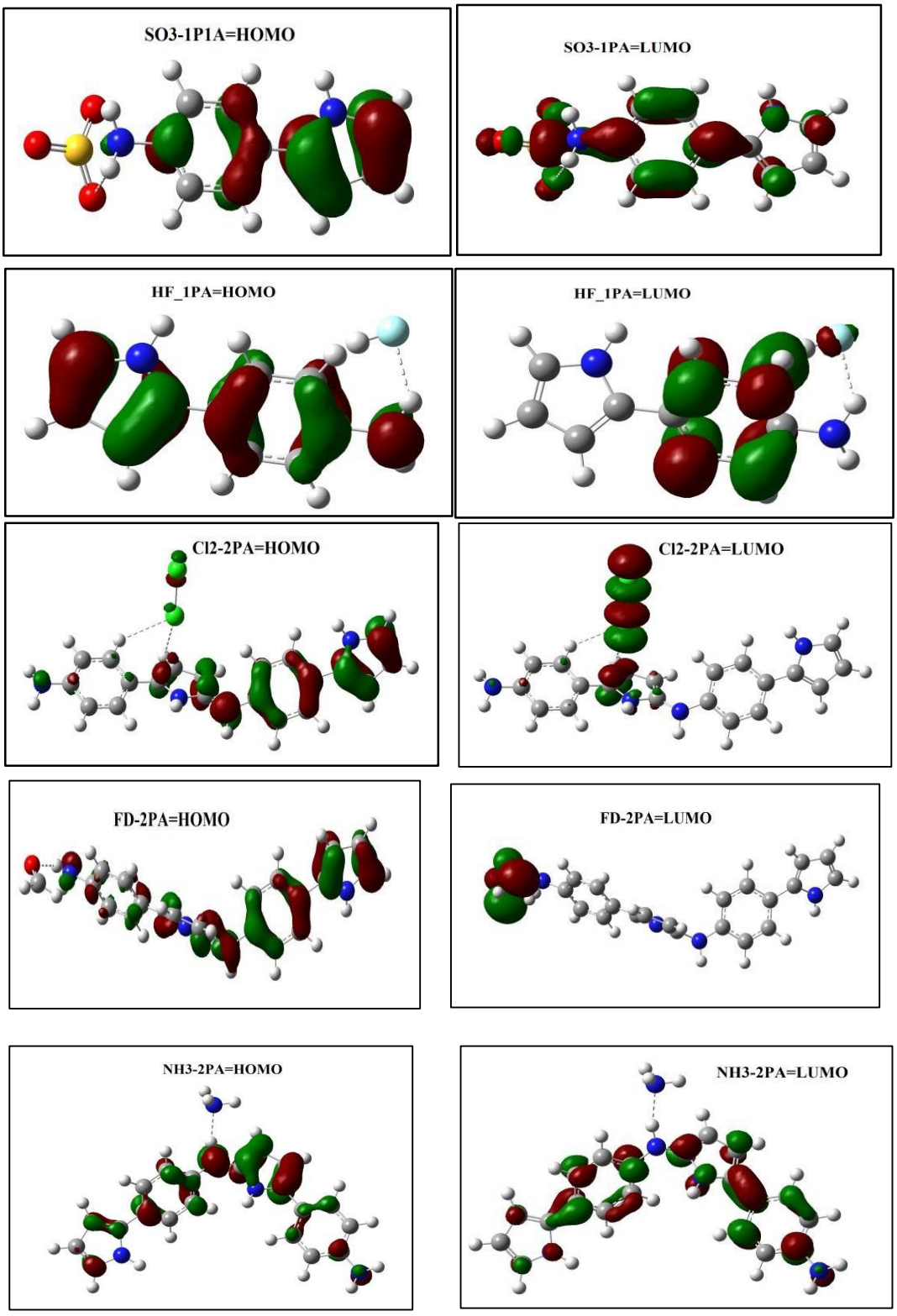
SO3-1P1A=HOMO
SO3-1PA=LUMO
HF_1PA=HOMO
HF_1PA=LUMO
Cl2-2PA=HOMO
Cl2-2PA=LUMO
FD-2PA=HOMO
FD-2PA=LUMO
NH3-2PA=HOMO
NH3-2PA=LUMO

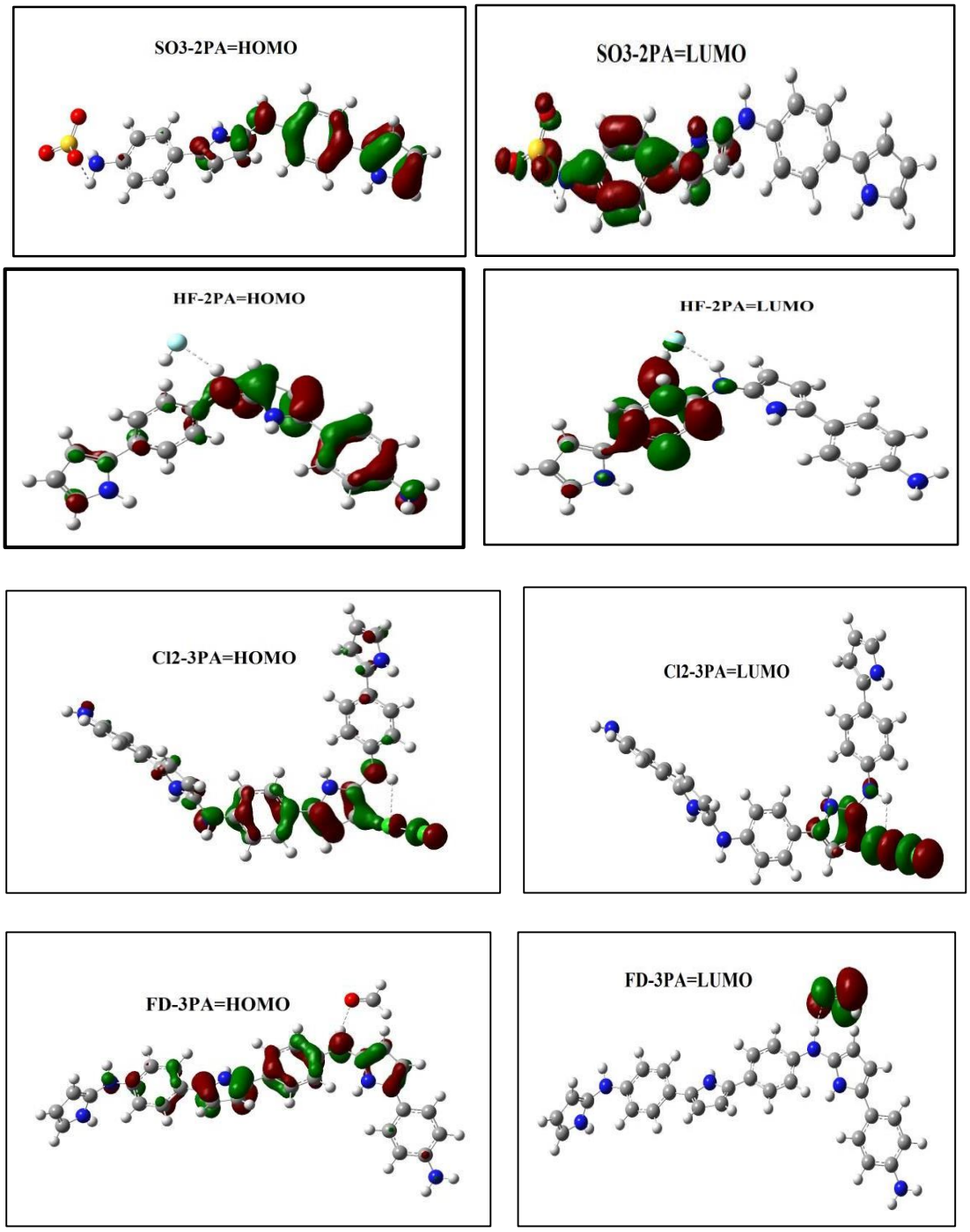
SO3-2PA=HOMO
SO3-2PA=LUMO
HF-2PA=HOMO
HF-2PA=LUMO
Cl2-3PA=HOMO
Cl2-3PA=LUMO
FD-3PA=HOMO
FD-3PA=LUMO

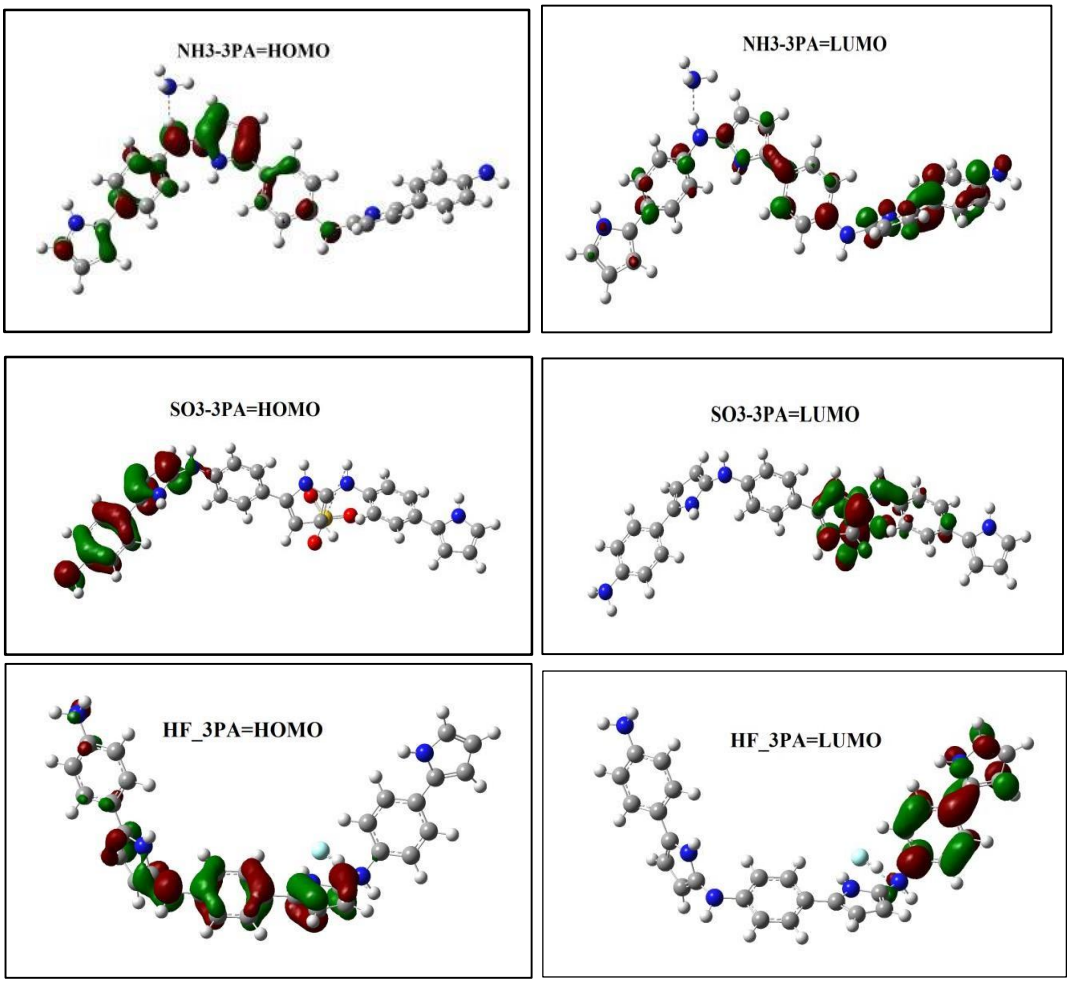

Figure 3. HOMO-LUMO structures of PA complexes

UV-Vis spectroscopic study

For sensing purpose, we might determine the variation in absorption properties. These variations give significant knowledge about the conductivity and sensing phenomena. UV-Vis analysis carried out for this purpose and results are obtained which includes oscillator strength (*f*) λ max (nm/ev) are represented in Table.7 Graphs are drawn by using origion software. Which are shown in Fig. (13, 14, 15, 16, 17), represents change in absorption properties. Due to maximum overlapping of wave function when isolated, PA interacts with analyte due to which the change in oscillator strength occurs. Similarly, maximum absorption is of the utmost importance for sensitivity [23]. After complexes formation conductivity and conjugation of the material increases. As a result,

Table 5 UV-Vis spectroscopic results of analytes, isolated PA and its complexes

		λ max (nm)	λ max (ev)	Ƒ	ΔE (ev) λmax shifting	Result
S#	**Analytes**					
1	**Chlorine (Cl_2)**	340.741	3.639	0	-	-
2	**Farmaldehyde(FD)**	134.744	9.201	0.106	-	-
3	**Amonia(NH_3)**	127.045	9.759	0.031	-	-

4	**Sulphertrioxide (SO_3)**	553.845	2.239	0.001	-	-
5	**HF**	81.144	15.280	0.313	-	-
	Isolated copolymer	**λ max (nm)**	**λ max (ev)**	**ƒ**	**ΔE (ev) λmax shifting**	**Result**
6	**Pyrrole-aniline monomer(1PA)**	274.025	4.5244	0.638	-	-
7	**Pyrrole-aniline dimer(2PA)**	300.514	4.126	0.072	-	-
8	**Pyrrole-aniline trimer(3PA)**	309.645	4.004	1.013	-	-
	1PA Complexes	**λ max (nm)**	**λ max (ev)**	**ƒ**	**ΔE (ev) λ max shifting**	**Result**
9	**Cl_2@1PA**	509.631	2.432	0.282	-2.092	**Blue Shift**
10	**FD@1PA**	299.0904	4.1453	0.0003	-0.3787	**Blue Shift**
11	**NH_3@1PA**	273.7792	4.5286	0.689	0.0046	**Red Shift**
12	**SO_3@1PA**	312.7641	3.9641	0.5883	-0.5599	**Blue Shift**
13	**HF@1PA**	277.662	4.4652	0.628	-0.0588	**Blue Shift**
	2 PA Complexes					
14	**Cl_2@2PA**	562.924	2.2025	0.1345	-1.9235	**Blue Shift**
15	**FD@2PA**	498.5142	2.4870	0.0005	-1.6390	**Blue Shift**
16	**NH_3@2PA**	346.7711	3.5753	0.7419	-0.5507	**Blue Shift**
17	**SO_3@2PA**	322.7424	3.8415	0.7478	-0.2845	**Blue Shift**
18	**HF@2PA**	318.668	3.8906	0.4175	-0.2354	**Blue Shift**
	3 PA Complexes					
19	**Cl_2@3PA**	551.9957	2.2461	0.2622	-1.7579	**Blue Shift**
20	**FD@3PA**	363.7373	3.4086	1.3549	-05954	**Blue Shift**
21	**NH_3@3PA**	353.4239	3.508	1.0041	0.496	**Blue Shit**
22	**SO_3@3PA**	395.3729	3.1358	0.1386	0.8682	**Blue Shift**
23	**HF@3PA**	333.7715	3.7146	0.2013	-0.2894	**Blue Shift**

maximum absorbance shifted to maximum wave length.by means of TD-DFT level of theory at B3LYP/6- 31 G (d) we simulated the UV-Vis spectra of isolated PA, analytes, and their complexes. From the data listed in Table 5 revealed that isolated 1PA, 2PA and 3PA shows maximum absorption values of 4.524, 4.126 and 4.004ev respectively., it becomes apparent that, upon interaction of analytes with 1PAcomplexes, Cl2@1PA (-2.092ev), FD@1PA (–0.3787ev) SO3@1PA (-0.5599 (ev) and HF@1PA (-0.0588 (ev) λ max values render blue shift and NH3@1PA **(**0.0046ev) follows red shift as a result of to π-π* transition.

The sensing capability of 1PA towards analytes can be scrutinized by these red and blue shifts. The values of λ max shift for Cl2@2PA**,** FD@2PA, NH3@2PA, SO3@2PA, and HF@2PA are -1.9235, -1.639, -0.5507, - 0.2845, -0.2845 and -0.2354ev, likewise for Cl2@3PA**,** FD@3PA, NH3@3PA, SO3@3PA, and HF@3PA are - 1.7579, -05954, -0.496, -0.8682, and -0.2894ev, respectively. and blue shifted exhibits by λ max values of all prior mentioned complexes. In addition, the prominent blue shift against SO3@PA complexes in compliance with its elevated interaction energy values as compare to rest of analytes, SO3@3PA produced the maximum shift with all PA (1PA, 2PA, 3PA) band gap decreases shows conformity of high sensitivity and high conductivity then other counterparts.Fig.(13,14,15,16,17) shows HOMO-LUMO distribution which is evidence of above mentioned fact.

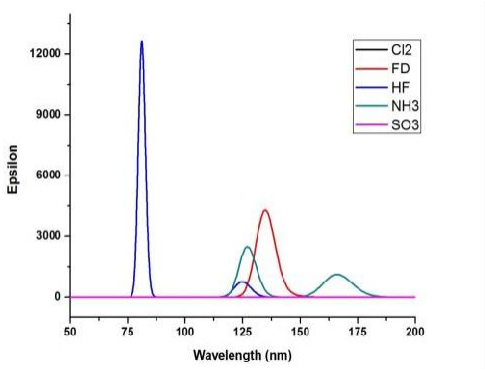

Fig 4. Graphical representation of interaction energies of analytes

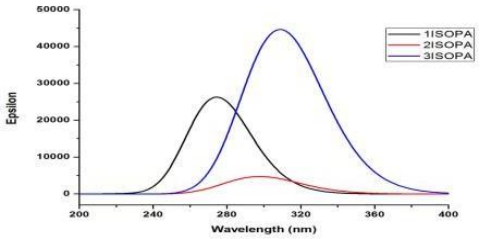

Fig 5. Graphical representation of interaction energies of isolated PA

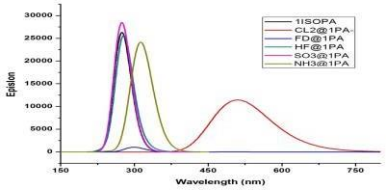

Fig 6. Graphical representation of interaction energies of analytes@1PA Complexes

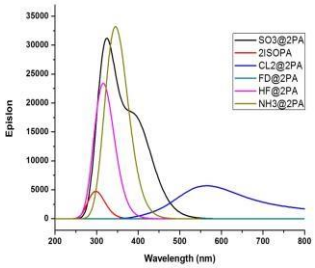

Fig 7. Graphical representation of interaction energies of analytes@2PA Complexes.

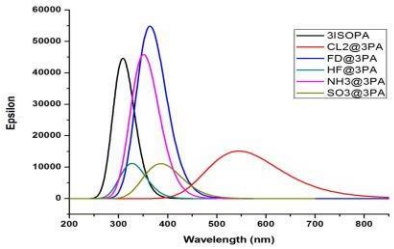

Fig 8. Graphical representation of interaction energies of analytes@3PA Complexes

`

Conclusions

The sensing ability of pyrroleaniline oligomers toward volatile organic compounds (VOCs) analytes is investigated. For this purpose, DFT studies of isolated and analytes doped pyrroleaniline oligomers are performed. The interaction energy between nPA and nPA@X (Cl2, NH3, SO3, CH2O and HF) is calculated at B3LYP-CP/6-31G (d). The trend of increasing interaction energy is: nPA-SO3 > nPA-HF > nPA-Cl2 > nPA- NH3 > nPA-CH2O. The interaction energies of Npa with SO3 are higher compared to those with HF, Cl2, CH2O and NH3. The difference in interaction energies arises due to the ionic nature of SO3 compared to the neutral nature of HF, Cl2, CH2O and NH3. After complexation with analytes (SO3, HF, Cl2, CH2O and NH3), the electronic and geometric parameters of pyrroleaniline oligomers change, illustrating the sensing ability of co-pPA toward analytes. However, the change in geometry is more prominent with SO3followed by HF, Cl2, CH2O and NH3, respectively. The charge transfers also revealed the interaction between co- pPA and analytes (SO3, HF, Cl2, CH2O and NH3). As the size of oligopyrroleaniline increases, the amount of charge transferred also increases. However, there is a greater amount of charge transfer in the case of nPA@SO3 and nPA@HF compared to nPA@NH3, nPA@CH2O and nPA@Cl2. In nPA@NH3, nPA@CH2O and nPA@Cl2 analytes doped oligopyrroleaniline, the charge is transferred from analyte to polymer, whereas in NH3, HF and CH2O, the charge is transferred from polymer to analyte. The energy gap of nPA decreases tremendously after interaction with SO3, HF, Cl2, CH2O and NH3, which results in increases in conductance. The lowest energy gap is observed in nPA@CH2O which is in the range of 1.00 to 1.86 eV. The trend of decrease of energy gap in different analytes doped polypyrroleaniline is: nPA@CH2O > nPA@NH3 > nPA@Cl2 > nPA@HF > nPA@SO3. The blue shift (in UV-visible spectra) occurs when nPA interacts with all five analytes. These results indicate the sensing ability of oligopyrroleaniline toward analytes (SO3, HF, Cl2, CH2O and NH3). Strong interaction in nPA@SO3is also justified from the IR spectroscopic results, where N−O stretching of analyte and N−H stretching of polymer in nPA@SO3− decrease, illustrating the strong interaction between oligopyrrole and analyte. The strong interaction is because each of the oxygen atoms of analyte (SO3) form hydrogen bonds with the hydrogen of oligopyrrole. All these parameters confirmed that doping of VOCs analytes on oligopyrroleaniline increases the sensing capability of polypyrroleaniline. Simultaneously, elongation of chain length also has a pronounced effect on the increasing sensitivity of pyrroleaniline toward analytes. Conclusively, all these results indicate the greater sensitivity of these pyrroleaniline oligomers toward VOCs although the highest interaction energy is calculated for the sulphur trioxide (SO3)

References

[1] Hu, H., J. Fine, P. Epstein, K. Kelsey, P. Reynolds, and B. Walker. (1989) Tear gas—harassing agent or toxic chemical weapon? Jama. 262(5): 660-663.

[2] Sajid, H., T. Mahmood, and K. Ayub. (2018) High sensitivity of polypyrrole sensor for uric acid over urea, acetamide and sulfonamide: a density functional theory study. Synthetic Metals. 235: 49-60.

[3] György, I., Conducting polymers: A new era in electrochemistry. 2008: Springer.

[4] Lakard, B., L. Ploux, K. Anselme, F. Lallemand, S. Lakard, M. Nardin, and J.-Y. Hihn. (2009) Effect of ultrasounds on the electrochemical synthesis of polypyrrole, application to the adhesion and growth of biological cells. Bioelectrochemistry. 75(2): 148-157.

[5] Trojanowicz, M. (2003) Application of conducting polymers in chemical analysis. Microchimica Acta. 143: 75-91.

[6] Huang, L., X. Zhuang, J. Hu, L. Lang, P. Zhang, Y. Wang, X. Chen, Y. Wei, and X. Jing. (2008) Synthesis of biodegradable and electroactive multiblock polylactide and aniline pentamer copolymer for tissue engineering applications. Biomacromolecules. 9(3): 850-858.

[7] Kesik, M., H. Akbulut, S. Söylemez, Ş.C. Cevher, G. Hızalan, Y.A. Udum, T. Endo, S. Yamada, A. Çırpan, and Y. Yağcı. (2014) Synthesis and characterization of conducting polymers containing polypeptide and ferrocene side chains as ethanol biosensors. Polymer Chemistry. 5(21): 6295-6306.

[8] Petr, A., F. Zhang, H. Peisert, M. Knupfer, and L. Dunsch. (2004) Electrochemical adjustment of the work function of a conducting polymer. Chemical Physics Letters. 385(1-2): 140-143.

[9] Garner, B., A. Georgevich, A. Hodgson, L. Liu, and G. Wallace. (1999) Polypyrrole–heparin composites as stimulus-responsive substrates for endothelial cell growth. Journal of biomedical materials research. 44(2): 121-129.

[10] Kim, D.H., S.M. Richardson-Burns, J.L. Hendricks, C. Sequera, and D.C. Martin. (2007) Effect of immobilized nerve growth factor on conductive polymers: electrical properties and cellular response. Advanced Functional Materials. 17(1): 79-86.

[11] Castano, H., E.A. O'Rear, P.S. McFetridge, and V.I. Sikavitsas. (2004) Polypyrrole thin films formed by admicellar polymerization support the osteogenic differentiation of mesenchymal stem cells. Macromolecular bioscience. 4(8): 785-794.

[12] Lee, J.-W., F. Serna, J. Nickels, and C.E. Schmidt. (2006) Carboxylic acid-functionalized conductive polypyrrole as a bioactive platform for cell adhesion. Biomacromolecules. 7(6): 1692-1695.

[13] Mingyin, C., Z. Zhang, S. Kong, and T. Miyake. H+-mediated control of biochemical processes in living organelles with electrochemical pH modulation. in The Proceedings of JSME annual Conference on Robotics and Mechatronics (Robomec) 2018. 2018. The Japan Society of Mechanical Engineers.

[14] Berneth, H. (2000) Azine dyes. Ullmann's Encyclopedia of Industrial Chemistry.

[15] Yin, X., H.T. Chung, U. Martinez, L. Lin, K. Artyushkova, and P. Zelenay. (2019) PGM-free ORR catalysts designed by templating PANI-type polymers containing functional groups with high affinity to iron. Journal of The Electrochemical Society. 166(7): F3240.

[16] Bennett, S., A history of control engineering, 1930-1955. 1993: IET.

[17] Banica, F.-G., Chemical sensors and biosensors: fundamentals and applications. 2012: John Wiley & Sons.

[18] Wali, R.P. (2012) An electronic nose to differentiate aromatic flowers using a real-time information-rich piezoelectric resonance measurement. Procedia Chemistry. 6: 194-202.

[19] Schöning, M.J. and A. Poghossian. (2002) Recent advances in biologically sensitive field-effect transistors (BioFETs). Analyst. 127(9): 1137-1151.

[20] Ratcliffe, N.M. (1990) Polypyrrole-based sensor for hydrazine and ammonia. Analytica chimica acta. 239: 257-262.

[21] Rabias, I. and B. Howlin. (2001) A combined ab initio and semi-empirical study on the theoretical vibrational spectra and physical properties of polypyrrole. Computational and Theoretical Polymer Science. 11(3): 241-249.

[22] Ullah, H., K. Ayub, Z. Ullah, M. Hanif, R. Nawaz, and S. Bilal. (2013) Theoretical insight of polypyrrole ammonia gas sensor. Synthetic metals. 172: 14-20.

[23] Ullah, H., A.-u.-H.A. Shah, S. Bilal, and K. Ayub. (2013) DFT study of polyaniline NH3, CO2, and CO gas sensors: comparison with recent experimental data. The Journal of Physical Chemistry C. 117(45): 23701-23711.

[24] Pal, R., S.L. Goyal, I. Rawal, and S. Sharma. (2020) Efficient room temperature methanol sensors based on polyaniline/graphene micro/nanocomposites. Iranian Polymer Journal. 29: 591-603.

[25] Bhadra, S. and D. Khastgir. (2008) Determination of crystal structure of polyaniline and substituted polyanilines through powder X-ray diffraction analysis. Polymer Testing. 27(7): 851-857.

[26] Frisch, M. (2009) gaussian 09, Revision d. 01, Gaussian. Inc, Wallingford CT. 201.

[27] Chen, S., S. Scheiner, T. Kar, and U. Adhikari. (2012) Theoretical study on relationship between structure of mercapto-triazole derivatives and inhibition performance. International Journal of Electrochemical Science. 7(8): 7128-7139.

[28] Ahmad, S.M., S. Bibi, S. Bilal, and K. Ayub. (2015) Spectral and electronic properties of π-conjugated oligomers and polymers of Poly (o-chloroaniline-co-o-toluidine) calculated with density functional theory. Synthetic Metals. 205: 153-163.

[29] Bibi, S., H. Ullah, S.M. Ahmad, A.-u.-H. Ali Shah, S. Bilal, A.A. Tahir, and K. Ayub. (2015) Molecular and electronic structure elucidation of polypyrrole gas sensors. The Journal of Physical Chemistry C. 119(28): 15994-16003.

[30] Kaloni, T.P., G. Schreckenbach, and M.S. Freund. (2016) Band gap modulation in polythiophene and polypyrrole-based systems. Scientific reports. 6(1): 36554.

[31] Hutchison, G., Y.-J. Zhao, B. Delley, A. Freeman, M. Ratner, and T. Marks. (2003) Electronic structure of conducting polymers: Limitations of oligomer extrapolation approximations and effects of heteroatoms. Physical Review B. 68(3): 035204.